The ISME Journal, 2025, **19(1)**, wraf131
https://doi.org/10.1093/ismejo/wraf131
Advance access publication: 26 June 2025
Original Article

Microbial cross-feeding stabilized by segregation of a dependent mutant from its independent ancestor

Olivia F. Schakel[1], Ryan K. Fritts[1,2], Anthony J. Zmuda[1,3], Sima Setayeshgar[4,*], James B. McKinlay[1,*]

[1]Department of Biology, Indiana University, Bloomington, IN 47405, United States
[2]Present address: Department of Molecular, Cellular and Developmental Biology and Cooperative Institute for Research in Environmental Sciences, University of Colorado Boulder, Boulder, CO 80309, United States
[3]Present address: Department of Plant and Microbial Biology, University of Minnesota, Twin Cities, Saint Paul, MN 55108, United States
[4]Department of Physics, Indiana University, Bloomington, IN 47405, United States

*Corresponding authors. Sima Setayeshgar, Department of Physics, Indiana University, 727 E 3rd Street, Bloomington, IN 47405, USA. E-mail: simas@iu.edu; James B. McKinlay, Department of Biology, Indiana University, 1001 E 3rd Street, Bloomington, IN 47405, USA. E-mail: jmckinla@iu.edu

Abstract

Microbial gene loss is hypothesized to be beneficial when gene function is costly, and the gene product can be replaced via cross-feeding from a neighbor. However, cross-fed metabolites are often only available at low concentrations, limiting the growth rates of gene-loss mutants that are dependent on those metabolites. Here we define conditions that support a loss of function mutant in a three-member bacterial community of (i) N_2-utilizing *Rhodopseudomonas palustris* as an NH_4^+-excreting producer, (ii) N_2-utilizing *Vibrio natriegens* as the ancestor, and (iii) a *V. natriegens* N_2-utilizaton mutant that is dependent on the producer for NH_4^+. Using experimental and simulated cocultures, we found that the ancestor outcompeted the mutant due to low NH_4^+ availability under uniform conditions where both *V. natriegens* strains had equal access to nutrients. However, spatial structuring that increasingly segregated the mutant from the ancestor, while maintaining access to NH_4^+ from the producer, allowed the mutant to avoid extinction. Counter to predictions, mutant enrichment under spatially structured conditions did not require a growth rate advantage from gene loss and the mutant coexisted with its ancestor. Thus, cross-feeding can originate from loss-of-function mutations that are otherwise detrimental, provided that the mutant can segregate from a competitive ancestor.

Graphical abstract

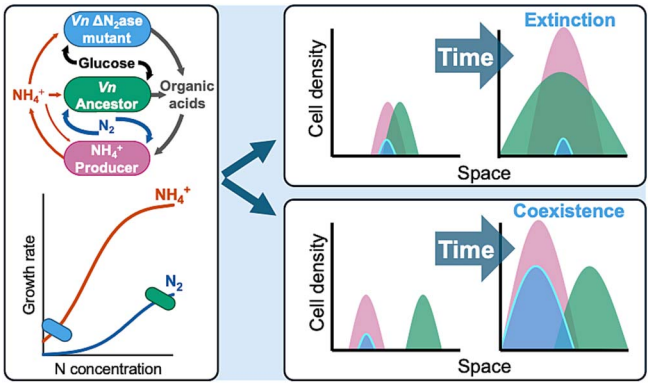

Keywords: cross-feeding; microbial interactions; *Rhodopseudomonas palustris*; *Vibrio natriegens*; Black Queen Hypothesis; mutualism; excretion; microbial physiology; gene loss; syntrophy

Introduction

Individuals within microbial communities constantly adapt to changing environments. One adaptation is beneficial loss-of-function (LOF) mutations, which are enriched (increase in frequency relative to the ancestor) when the cost of losing a gene is outweighed by the benefit of acquiring the gene product from a neighbor. This type of gene loss is perhaps best known as the Black Queen Hypothesis (BQH) [1, 2]. The BQH includes a "producer" that creates a public good that promotes beneficial gene loss in a recipient "beneficiary" [1, 2]. The term distinguishes beneficiaries

Received: 25 January 2025. **Revised:** 20 May 2025. **Accepted:** 25 June 2025

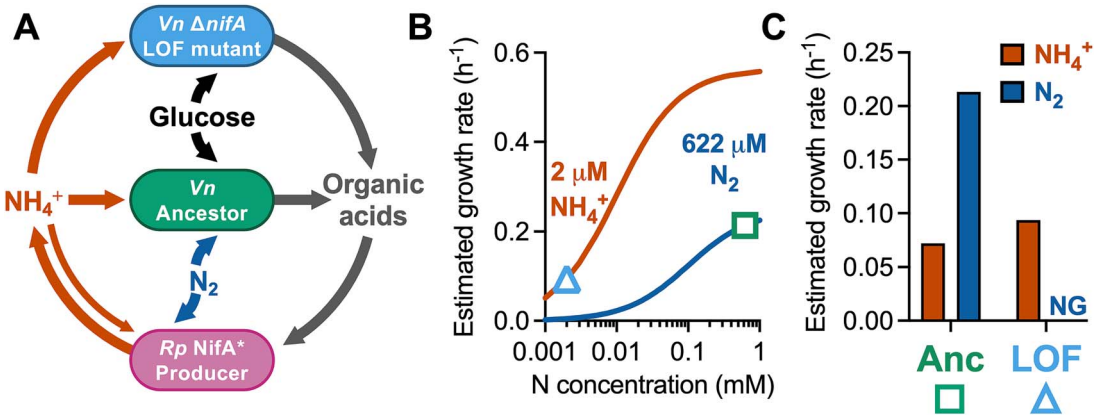

Figure 1. The LOF mutant growth rate is inferior to that of the ancestor due to the low concentration of cross-fed nutrient; (A) the coculture consists of (i) a producer, *R. palustris* (*Rp*) that fixes N_2 and excretes NH_4^+ due to a NifA* mutation, and two *V. natriegens* (*Vn*) strains consisting of, (ii) a recipient that is incapable of N_2 fixation and depends on the producer for NH_4^+, and (iii) a self-sufficient, N_2-fixing ancestor; all strains are non-motile; (B) Monod model estimates of *V. natriegens* ancestor and mutant growth rates in the coculture based on the concentration of each nitrogen source (symbols); despite a higher maximum growth rate possible with NH_4^+, sub-saturating NH_4^+ concentrations dictate that the ancestor will grow faster with N_2 (square) than the mutant with NH_4^+ (triangle); see the Methods for model details; (C) estimated ancestor and recipient growth rates in coculture with each nitrogen source.

from mutants with neutral or detrimental LOF mutations. Beneficiaries also do not harm the producer, distinguishing them from LOF "cheaters" that gain an adaptive advantage by exploiting public goods at the expense of the producer [1, 3, 4]. The fitness advantage from the LOF mutation should lead to the extinction of the ancestral strain, provided that the producer is another species [1]. Adaptive gene loss supported by cross-feeding has been used to explain the natural prevalence of LOF mutants, like auxotrophs [5–9]. However, whereas nutrient-rich conditions are known to enrich for auxotrophs [10–13] and cross-feeding of molecules like iron-scavenging siderophores can enrich for cheaters [14–16], there are few direct observations of long-term cross-feeding leading to the enrichment of spontaneously-evolved LOF beneficiaries [17, 18]; most studies used engineered LOF mutants.

One reason why gene loss might be infrequently observed is because cross-fed nutrients often exist at sub-saturating concentrations, preventing the mutant from achieving a maximum growth rate theoretically afforded by gene loss (Fig. 1). For example, a trait that was predicted to be subject to beneficial gene loss is N_2 fixation, the conversion of nitrogen gas (N_2) into ammonium (NH_4^+) via the cytoplasmic enzyme nitrogenase [1, 2]. N_2 fixation is essential, expensive (e.g. 16 ATP per N_2 fixed [19]), and NH_4^+ can passively escape the cell due to its equilibrium with membrane-permeable NH_3 [19–22]. However, when we cocultured NH_4^+-requiring *Escherichia coli* with wild-type (WT) N_2-fixing *Rhodopseudomonas palustris*, *E. coli* initially grew at <1% of the maximum possible rate and only reached 5% after 146 generations [22]. When we engineered *R. palustris* to excrete NH_4^+, *E. coli* still only grew at 25% or 43% of the maximum growth rate, depending on the level of NH_4^+ excretion [23]. Based on these observations, we predict that in the presence of an NH_4^+-excreting producer, another N_2-fixing bacterium would have a competitive advantage over a daughter nitrogenase LOF mutant (Fig. 1A), whose growth rate would be restricted by low NH_4^+ availability (Fig. 1B, C).

Development and maintenance of cross-feeding is also observed in spatially structured populations [5, 24–30]. Community structure can create nutrient pockets, deserts, and gradients where populations have differential access based on local conditions [30–33]. Clustering of cooperating partners can decrease local nutrient concentrations, keeping cheaters to the fringes [24, 27, 29, 34–36]. Metabolite-externalizing populations can also achieve larger populations, despite carrying costly mutations, when physically aggregated within cross-feeding communities [28, 29]. More broadly, spatial structure can accommodate diversity [37], including cheaters [24, 29] and other competitors [38], but also slow-growing subpopulations derived from an ancestor [33, 39]. These less-fit mutants can succeed at the edges of a competitive ancestor population [39], an important aspect of Wright's shifting balance theory on how small populations can navigate fitness valleys [40]. Thus, the extent to which fitness advantages from LOF mutations are necessary for survival or enrichment in structured environments remains unclear.

Here we address conditions that can support the enrichment of a nitrogenase LOF mutant as a proxy for emergence in nature. We used a defined bacterial community resembling one that could result in a BQH scenario to test whether the LOF mutant would be enriched as a beneficiary, cheater, or a mutant without a fitness advantage. The community consisted of two species, where one was an NH_4^+-excreting producer, and the other species was subdivided into a self-sufficient ancestor and a LOF mutant that was dependent on the producer (Fig. 1). Using both experimental cocultures and computational models, we found that the LOF mutant was always outcompeted by the ancestor under uniform conditions. However, by progressively limiting population overlap, we identified spatial conditions wherein partial segregation allowed the LOF mutant to coexist with the ancestor, independently of any advantage afforded by the LOF mutation. Our results thus indicate that spatial structuring of populations can sustain LOF mutants without meeting BQH criteria of ancestor extinction nor a LOF mutation imparting a fitness advantage.

Materials and methods

Bacterial strains

Strains, plasmids, and primers are in Tables S1–S3. Mutations were verified via Sanger sequencing. *Vibrio natriegens* strains

were derived from TND1964, containing pMMB-tfoX [41] (WT). *V. natriegens* mutations were made by introducing linear PCR products via natural transformation [41, 42]. The "ancestor," OFS003, is a kanamycin resistant (Δ*dns*::Kan^R), non-motile (Δ*flgE*; flagellar hook) derivative of the WT strain (Fig. S1). The LOF mutant, OFS004, additionally carries a Δ*nifA* mutation, preventing N_2 fixation, and *dns* is instead replaced by a spectinomycin resistance cassette. Each cassette had a comparable effect on the growth rate (Fig. S2).

The "producer," *R. palustris* CGA4067, is a non-motile derivative of CGA4005 [43], which itself is derived from type strain CGA0092 [44]. CGA4067 is incapable of H_2 oxidation (Δ*hupS*), has low cell aggregation (Δ*uppE*) [45], excretes NH_4^+ due to a mutation in *nifA* [46], and is non-motile due to deletion of *motAB* (flagella stator). CGA4039 was made incapable of N_2 fixation by deleting structural genes for all three nitrogenase isozymes [47]. *R. palustris* deletion mutations were made by homologous recombination after introducing the appropriate suicide vector [47, 48], via electroporation [23, 49, 50].

Growth conditions

V. natriegens and *R. palustris* were recovered from 25% glycerol frozen stocks (-80°C) on agar plates containing LB3 (lysogeny broth with 2% w/v NaCl) for *V. natriegens* or photosynthetic media (PM) [51] with 10 mM disodium succinate for *R. palustris*. Kanamycin (100 μg ml^{-1}) or spectinomycin (200 μg ml^{-1}) were included where appropriate. Anoxic media was prepared by bubbling with N_2 in culture vessels, then sealing with rubber stoppers and aluminum crimps prior to autoclaving. Starter cultures were grown from single colonies in 27-ml anaerobic tubes with 10 ml of minimal media. *R. palustris* was grown in M9-derived coculture media (MDC) [23] with 1.5 mM disodium succinate. *V. natriegens* was grown in MDC modified with (final concentrations): 10 mM glucose, 80 mM NaCl, 200 mM MOPS (pH 7), and 0.5 mM NH_4Cl, to transition cells to N_2-fixing conditions; this media, without NH_4Cl, is called VMDC. A 1% inoculum of *R. palustris* and a 0.5% inoculum of each *V. natriegens* strain was then used to start anoxic cocultures in VMDC with 5 mM glucose. Cultures were incubated at 30°C with light from a halogen bulb (750 lumens).

Shaken (150 RPM) cocultures, including for invasion-from-rare (IFR) assays, were grown in 10-ml volumes in 27-ml tubes, oriented horizontally. Static IFR assays were performed in 4-ml volumes in 10-ml anoxic serum vials with or without agarose (Research Products International). Contaminating nitrogen was removed from agarose (Fig. S3) by washing 0.15 g of agarose twice with ultra-pure water and then once with VMDC (12-ml volumes in a 15-ml conical tube; agarose was pelleted by centrifuging at 2415 × g and removing supernatants by pipette). Washed agarose was resuspended in 100 ml VMDC in a 160-ml serum vial before making anoxic and autoclaving. After autoclaving, molten agarose was kept suspended during cooling by rocking overnight (Boekel Scientific). Agitated agarose was stirred with a stir bar overnight during cooling (200 RPM). Glucose and cations were added and then agarose media was dispensed into serum vials by syringe using a 1″, 23-gauge needle (BD). IFR assays were inoculated with 9 × 10^6 cells of producer and 9 × 10^6 cells of LOF mutant plus ancestor at the specified ratio. For randomized static cell distributions, the inoculum was dropped onto the media and allowed to settle during incubation. Localized populations were inoculated on opposite sides of the vial using a 2″, 21-gauge needle (BD), to slowly inject cells just below the surface, without touching the glass.

Analytical procedures

Motility was determined by using a pipette tip to stab a single colony into LB3 with 0.3% agar and then measuring swim diameter 17 h later. Cell density was measured as optical density at 660 nm (OD_{660}) using a Genesys 20 spectrophotometer (Thermo-Fisher) or colony-forming units (CFUs) on selective media (see above). Growth rates were determined by fitting an exponential trendline using Microsoft Excel. Glucose, organic acids, and ethanol were quantified using a Shimadzu high performance liquid chromatograph as described [52]. For IFR assays, initial cell densities in agarose were assumed to be the same as those determined in 0.3 ml samples from liquid controls. Final cell densities, and metabolite levels were determined after 6 days by vortexing vials and then sampling 1 ml. For location sampling, 0.35 ml was taken using a 2″, 21-gauge needle; cultures were then discarded. LOF mutant change in frequency $\Delta f = (\text{LOF}/(\text{LOF}+\text{ancestor}))_{\text{final}} - (\text{LOF}/(\text{LOF}+\text{ancestor}))_{\text{initial}}$ [53], where each LOF and ancestor population was determined by counting CFUs or using the reported populations from simulations. Linear regression for IFR assays and other statistical analyses were performed using GraphPad Prism v10. The extrapolated *x*-intercept was used to infer the competitive outcome between the LOF mutant and the ancestor as: (x,0) between 0 and 1, coexistence; $(x,0) \geq 1$, ancestor extinction; $(x,0) \leq 0$, mutant extinction.

Mathematical modeling

The Monod model (Fig. 1) was:: $\mu = \mu_{max}\, S/(S + km)$, where: μ, growth rate; μ_{max}, maximum growth rate; S, NH_4^+ or N_2 concentration; km, half-saturation constant for S. Parameter values: NH_4^+, 2 μM based on 20 μM *R. palustris* OD_{660}^{-1} [23]; N_2, 622 μM based on Henry's law assuming 1.02 atm and N_2 solubility of 6.1× 10^{-4} M atm^{-1}) [54]; μ_{max} with NH_4^+, 0.43 h^{-1}; μ_{max} with N_2, 0.25 h^{-1}; km_{NH4+}, 0.01 mM [55]; km_{N2}, 0.1 mM [56]. A 1.3-fold μ_{max} advantage with NH_4^+ was assumed for the LOF mutant based on a comparison of *R. palustris* strains (Fig. S4).

Population and metabolic dynamics in cocultures were simulated in Mathematica (v13.3 Wolfram Research, Inc., 2023) using coupled, nonlinear reaction–diffusion equations modified from previous models describing cross-feeding between *R. palustris* and *E. coli* [23, 43]. We numerically simulated the equations subject to no-flux boundary conditions using Mathematica's NDSolve[] function employing a stiff solver. Default parameter values are given in Table S4. Cell densities, c_i, are in number of cells ml^{-1}, and the numerical solution corresponds to time-dependent concentrations in a system size of $(L_x = 2\ \text{cm}) \times (L_y = 2\ \text{cm}) \times (1\ \text{cm})$. The time evolution of cell densities in the $x - y$ plane is investigated under different conditions, assuming the concentrations in the z−direction are uniform. Diffusion constants for cells and nutrients in liquid media versus the agarose matrix were estimated using the Stokes-Einstein relation (Table S4). Model equations and details are available in the Supplementary material.

Results

Development of a coculture to test BQH predictions

Previously, we established obligate reciprocal cross-feeding between *E. coli* and an *R. palustris nifA*∗ mutant [46]; *E. coli* fermented glucose and excreted organic acids as essential carbon for *R. palustris* and *R. palustris* fixed N_2 and excreted NH_4^+ as essential nitrogen for *E. coli* [23]. N_2 fixation was predicted to be

subject to beneficial gene loss according to the BQH [1, 2]. To test whether loss of N_2 fixation would be beneficial to bacteria cocultured with NH_4^+-excreting *R. palustris*, we sought to replace *E. coli* with N_2-fixing, fermentative, *V. natriegens*. In the desired coculture, *V. natriegens* would comprise a self-sufficient "ancestor" subpopulation and a recipient LOF mutant subpopulation that is dependent on the *R. palustris* "producer" for NH_4^+ (Fig. 1A). We refrain from calling the LOF mutant a beneficiary unless we confirm a fitness benefit from the LOF mutation.

To build our desired populations, we prevented *V. natriegens* N_2 fixation by deleting *nifA*, encoding the transcriptional activator of nitrogenase genes. The Δ*nifA* LOF mutant did not grow with N_2 but showed similar growth kinetics to the parent (ancestor) in monocultures and in *V. natriegens* cocultures with NH_4Cl (Fig. S5; *R. palustris* omitted). We then verified that the producer could support the LOF mutant in coculture with N_2; population trends resembled *R. palustris* + *E. coli* cocultures, with both strains having a common exponential phase where the *V. natriegens* LOF growth rate more closely resembled that of *R. palustris nifA*∗ than a monoculture growth rate [23] (Fig. S6A, B versus Fig. S5B, C). In contrast, coculturing *R. palustris* with the *V. natriegens* ancestor resembled *R. palustris* + *E. coli* cocultures with NH_4Cl; rapid growth by the *V. natriegens* ancestor was followed by *R. palustris* growth [23] (Fig. S6C). Glucose was exhausted and organic acids accumulated in the first phase, indicative of *V. natriegens* ancestor growth, and then organic acids were depleted in the second phase, indicative of *R. palustris* growth (Fig. S6D). Having established the expected trends, we then examined cocultures comprised of the producer, ancestor, and LOF mutant (Fig. 1A).

The LOF mutant is not enriched when *V. natriegens* subpopulations have equal access to nutrients

Like cocultures pairing the producer and ancestor (Fig. S6C), shaken cocultures combining the producer, ancestor, and LOF mutant had two growth phases (Fig. 2A). Tracking (sub)populations by CFUs showed an early dominance by the LOF mutant. We assume that early LOF mutant growth was supported by trace organic nitrogen (3×10^6 cells ml^{-1} can be explained by 11 μM NH_4^+; Table S4) while the ancestor lagged, which we commonly observe when *V. natriegens* uses N_2. Trace nitrogen could include high nM - low μM NH_4^+ from *R. palustris* starter cultures and compounds from *V. natriegens* death upon transfer (note the low initial cell densities). However, this early advantage was brief, and the ancestor outcompeted the LOF mutant by 24 h (Fig. 2B). At that time, glucose was exhausted and both *Vibrio* strains enter stationary phase (Fig. 2C).

The above experiment used an initial LOF mutant frequency of ∼0.5, relative to the ancestor. To determine if the LOF mutant could be enriched from different initial frequencies we performed a reciprocal invasion-from-rare (IFR) assay, which also tests the mutual invasion criterion for coexistence [53, 57]. When trends are linear, an *x*-intercept (*x*,0) between 0 and 1 suggests coexistence of the mutant and ancestor, whereas $(x,0) \geq 1$ suggests ancestor extinction, and $(x,0) \leq 0$ suggests mutant extinction [53, 57, 58]. IFR assays provide similar insights as serial transfers but they can be performed more quickly and are less prone to evolution affecting the results [53]. We inoculated the LOF mutant and ancestor at variable frequencies in shaken cocultures keeping the total initial *V. natriegens* population at a 1:1 ratio with *R. palustris*. The LOF mutant was consistently outcompeted by the ancestor ($(x,0) = 0.01$, 95% CI: −0.19 to 0.14; Fig. 2D).

We considered that LOF mutant enrichment could be influenced by NH_4^+ excretion level (Fig. 1B, C) and the LOF mutant fitness advantage. To explore these parameters, we built upon a mathematical model [23] to describe population growth and diffusion of cells and nutrients over a 2 × 2 cm domain (Supplementary materials). First, we tested whether the model could replicate experimental trends by simulating IFR conditions with uniformly distributed populations and nutrients. We gave the LOF mutant a maximum growth rate (μ^b_{max}) advantage of 1.1-times that of the ancestor, based on a comparison of *R. palustris* growth rates with and without nitrogenase expression (Fig. S4); a similar comparison was not possible with *V. natriegens* because we do not have a mutant that expresses nitrogenase in the presence of NH_4^+. The results resembled those from experimental cocultures with an *x*-intercept that was not significantly different from zero (Fig. 2E).

We mapped what maximum growth rate (μ^b_{max}) advantage would be required for the LOF mutant to have a positive change in frequency (Δf) at different producer NH_4^+ excretion levels. At the experimentally-estimated NH_4^+ excretion level of 6.5×10^{-10} μmol $cell^{-1}$ [23], the LOF mutant would need an unrealistic 8-fold maximum growth rate advantage over the ancestor (Fig. 2F, circle). The LOF mutant could be enriched with a lower growth rate advantage at NH_4^+ excretion levels 1–2 orders of magnitude higher than *R. palustris nifA*∗ (Fig. 2F). Whereas a wide range of NH_4^+ excretion levels can be engineered [23, 59, 60], natural examples are within an order of magnitude of *R. palustris nifA*∗ excretion level (∼8.3×10^{-10} μmol $cell^{-1}$ for *Azotobacter* [61] assuming a cell weight of 1 pg [62]). We also considered a scenario where the producer grows as fast as the ancestor (instead of a ∼3-fold difference in growth rate), to yield more public NH_4^+. Using the higher producer growth rate shifted the Δf boundary in favor of LOF mutant enrichment, but the required growth advantage was still ∼3.5-times that of the ancestor at the experimentally estimated NH_4^+ excretion level (Fig. 2F).

We considered how NH_4^+ privatization might affect population outcomes. NH_4^+ from nitrogenase is highly privatized; N_2 fixation occurs in the cytoplasm where most NH_4^+ will be assimilated before it can escape. Generation of public goods outside the cell can profoundly affect producer–consumer relationships [2, 43, 63–65]. Low privatization can enrich for LOF cheaters [14, 34, 66–68] and thus might also enrich for LOF beneficiaries. To explicitly address low privatization, we modified our model to describe a hypothetical production of NH_4^+ outside of the cell by both N_2 fixing bacteria [43] (Fig. 3A). In this scenario, the LOF mutant was predicted to outcompete the ancestor, provided the LOF mutant had a growth rate advantage; an *x*-intercept could not be determined due to the nonlinear trend. However, every change in frequency was positive (Fig. 3B). Without the growth advantage, each change in frequency was zero (Fig. 3B). Thus, whereas our results suggest that N_2 fixation is unlikely to lead to the enrichment of LOF beneficiaries, the outcome could be different for less-privatized public goods. Moving forward, we focused on whether spatial structuring of populations might facilitate LOF nitrogenase mutant enrichment, despite high privatization.

Static conditions do not enrich for the LOF mutant

Spatially structured communities can foster populations that might otherwise have a fitness disadvantage [28, 29, 33, 38]. We thus tested whether spatial structuring could lead to nitrogenase LOF mutant enrichment. We began with minimal intervention by coculturing non-motile strains under static conditions in either

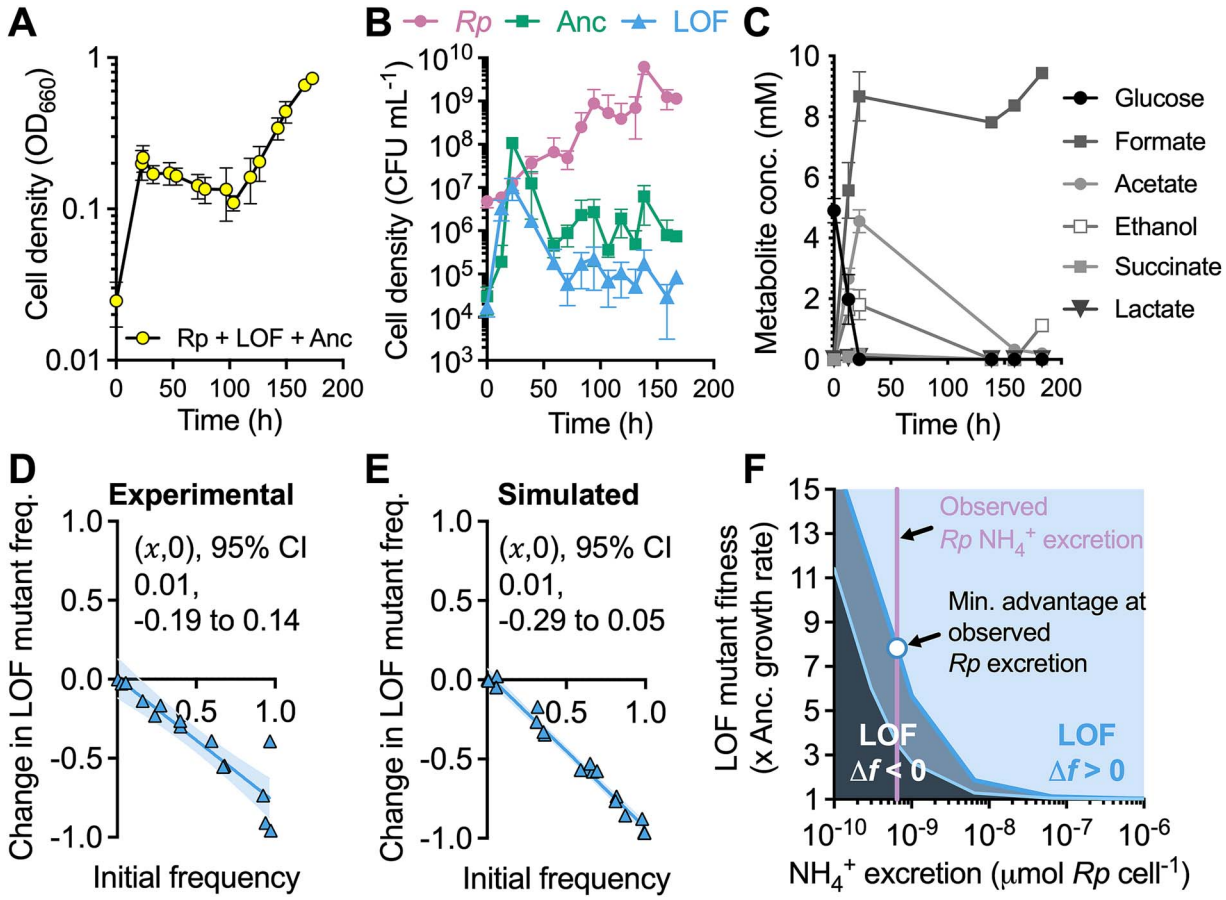

Figure 2. The ancestor outcompetes the LOF mutant in shaken cocultures; (A) growth of shaken cocultures of *R. palustris*, *V. natriegens* Δ*nifA* LOF mutant, and WT *V. natriegens* "ancestor;" (B) growth of each strain, determined using selective plating for CFUs; (C) glucose and fermentation product concentrations in cocultures; (A-C) points are means ± SD (n = 3); (D, E) IFR assays in shaken liquid experimental cocultures (D) or simulated cocultures with spatially uniform conditions (E); coexistence is assumed if the x-intercept (x,0) is between 0 and 1, otherwise it is assumed that one population drives the other to extinction; each point is a single experimental or simulated coculture; initial LOF mutant frequencies were the same for experimental and simulated cocultures (initial frequency range = 0.5%–97.3% using *V. natriegens* populations only); x-intercept and 95% CI error bands were determined using linear regression analysis; (F) boundaries where the LOF mutant change in frequency goes from negative ($\Delta f < 0$; extinction) to positive ($\Delta f > 0$; enriched) for different producer (*Rp*) NH_4^+ excretion levels and LOF mutant maximum growth rate (μ^b_{max}) values relative to the ancestor (Anc); LOF mutant initial frequency $f_0 = 0.061$; outer dark blue boundary line, results with observed producer maximum growth rate; inner light blue boundary line, results if producer maximum growth rate = ancestor maximum growth rate; purple vertical line, experimentally-estimated producer NH_4^+ excretion level; circle, minimum LOF mutant growth advantage required to avoid extinction at the experimentally-estimated producer NH_4^+ excretion level.

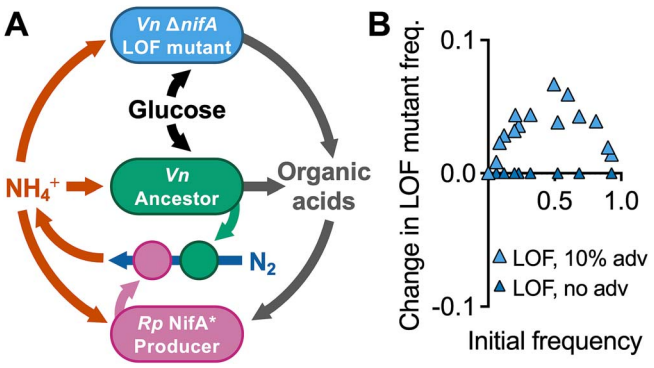

Figure 3. Hypothetical extracellular NH_4^+ production allows for enrichment of the LOF mutant in accordance with the BQH; (A) the modified model allows for production of NH_4^+ via a hypothetical extracellular enzyme (circles) produced by the N_2-fixing producer and ancestor populations; (B) simulated IFR with extracellular NH_4^+ production under spatially uniform conditions; initial LOF mutant frequency range = 0.1%–92.8% using *V. natriegens* populations only.

liquid or a fluid 0.15% agarose matrix (Fig. 4A); we assumed that random spatial structuring developed as the cells settled. Our IFR assays, sampled after mixing at the final time point, suggested that the LOF mutant would go extinct; both conditions gave x-intercepts that were not significantly different from zero (Fig. 4B). We also tested these conditions using the mathematical model with a random initial cell distribution and diffusion constants consistent with agarose, where appropriate (Table S4). The simulations also suggested LOF mutant extinction in both conditions (Fig. 4C).

Segregation leads to LOF mutant enrichment without a maximum growth rate advantage

Cross-feeding neighborhoods can occur at the scale of one to several cells [31]. Thus, although we did not observe LOF mutant enrichment at the domain level, there could have been pockets of local enrichment. We addressed this possibility using the model by varying a spatial filter (p) for the initial ancestor random distribution, while maintaining a spatial filter value for the initial

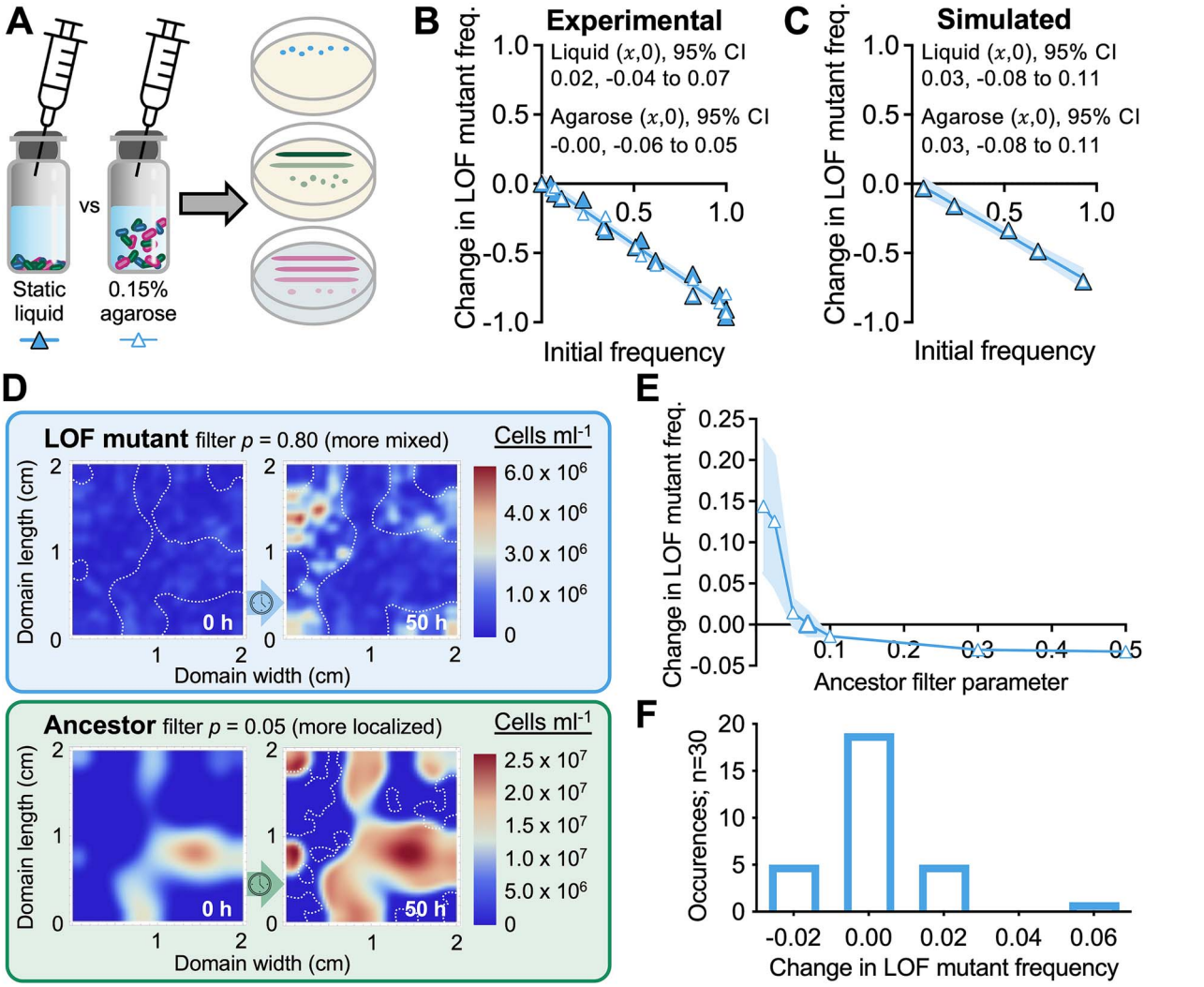

Figure 4. Segregation from ancestor populations can theoretically lead to local and domain-level enrichment of the LOF mutant; (A) experimental approaches to randomly distribute non-motile cells in static liquid cocultures without or with a fluid 0.15% agarose matrix; community composition was assessed after 6 days by selective plating; experimental (B) and simulated (C) IFR assays with randomized cell distributions in static liquid or 0.15% agarose; each point is from an individual experimental or simulated coculture; initial LOF mutant frequencies were the same for experimental and simulated cocultures (initial frequency range = 0.1%–99.9% using *V. natriegens* populations only); experimental IFR assays were only mixed before sampling; x-intercept and 95% CI error bands were determined using linear regression analysis; simulated agarose used lower diffusion coefficients; (D) simulated cell densities in a 2 × 2 cm domain (assumed to be uniform across height) at 0 h and 50 h; initial LOF mutant frequency f_0 was 0.061; initial random beneficiary and producer populations were specified using a common filter parameter ($p = 0.80$); the ancestor population was distributed using $p = 0.05$; dotted lines show the boundaries of where a competitor population is relatively high (compare top vs bottom graphs); (E) mean LOF mutant change in frequency ($\Delta f(t)$) from different random cell distributions (LOF mutant and producer given by $p = 0.80$ for all ancestor filter parameter values); n = 10 except the enlarged data point, where n = 30; error bands = SD; (F) histogram for the enlarged data point in (E) where the ancestor $p = 0.07$ (n = 30), and the LOF mutant change in frequency is ~0; this threshold change in frequency value is unique to these simulation parameters.

random LOF mutant and producer distributions ($p = 0.80$). Larger filter parameters give rise to a more fine-grained spatial variation, resulting in more mixing of populations (Fig. S7). Smaller filter parameters correspond to spatial coarsening ($p = 0.05$), creating regions where the ancestor is more isolated, though populations still overlap (Fig. S7). Simulations using $p = 0.05$ showed that the LOF-mutant can expand its population in regions where the ancestor population remained low (Fig. 4D). When averaged across the entire domain, the LOF mutant could be enriched when the initial ancestor distribution was coarse ($p \leq 0.07$; Fig. 4E, F).

We sought more control over the spatial distributions to address how partial segregation impacts population outcomes. We therefore simulated partially overlapping Gaussian distributions of each initial population at distinct sites (Fig. 5A; ancestor at (x = 0.5, y = 1 cm) and the LOF mutant and producer colocalized at (x = 1.5, y = 1 cm). Upon glucose depletion (~150 h), the ancestor had grown around the LOF mutant and producer populations, highlighting that the populations did not grow in compartmentalized isolation (Fig. 5A). Despite some spatial overlap of the initial Gaussian distributions, partial segregation led to LOF mutant enrichment ((x,0) = 0.38; 95% CI: 0.36 to 0.43), with predicted coexistence with the ancestor (Fig. 5B).

We constructed an experimental counterpart by inoculating populations at specific locations just below the surface of 0.15% agarose media (Fig. 5C). We first verified that populations were both localized and partially overlapping, using non-motile ancestor monocultures; the ancestor was detected at the opposite side of the vial by 20 h, spreading via diffusion and growth (Fig. 5D).

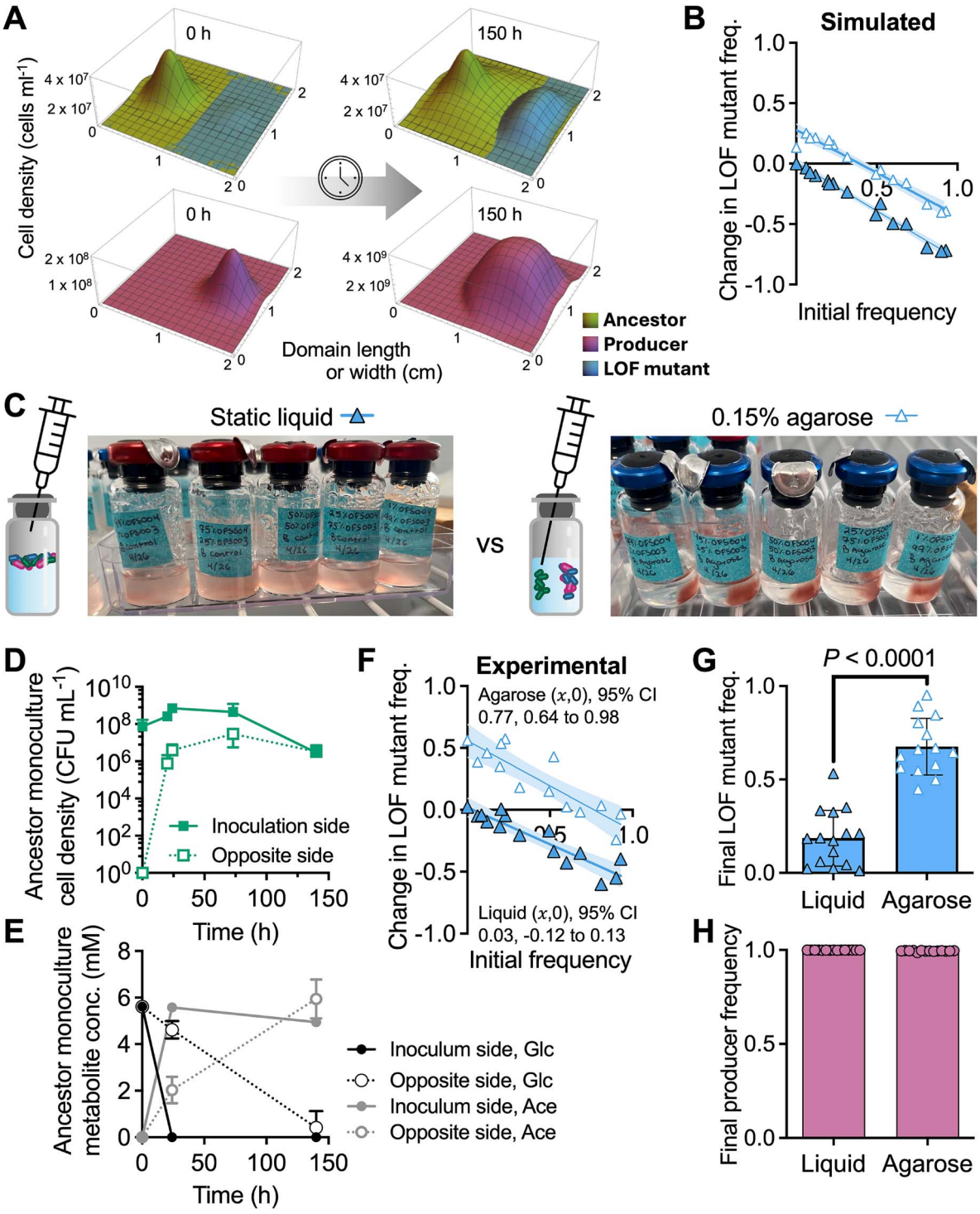

Figure 5. Colocalization with the producer and segregation from the ancestor leads to domain-level enrichment of the LOF mutant; (A) example of simulated Gaussian distributions of initial populations; the LOF mutant and the producer were colocalized but are shown on separate graphs for visualization purposes; cell densities are assumed to be uniform across height; different producer y-axis scales were used to make the initial population visible; (B) simulated IFR in liquid versus 0.15% agarose using the distinct inoculation sites in (A); (C) experimental cocultures were inoculated to static liquid or to locations in 0.15% agarose; localization is evident from pigmented *R. palustris* growth after 6 days; (D, E) cell densities (D) and glucose and acetate concentrations (E), inferred from samples taken at the inoculation site and at the opposite side of the vial in ancestor monocultures with 0.15% agarose; points are means ± SD, n = 3; (F) IFR from the experimental conditions; cocultures were only mixed before sampling (B, F) each point is from an individual experimental or simulated coculture; initial LOF mutant frequencies were the same for experimental and simulated cocultures (initial frequency range = 0.1%–92.7% using *V. natriegens* populations only); x-intercept and 95% CI error bands were determined using linear regression analysis; final LOF mutant frequency (G, using *V. natriegens* populations only) and the producer (H, using all populations) in static liquid or 0.15% agarose; bars are means ± SD, n = 15; *P* value is from a two-tail t-test.

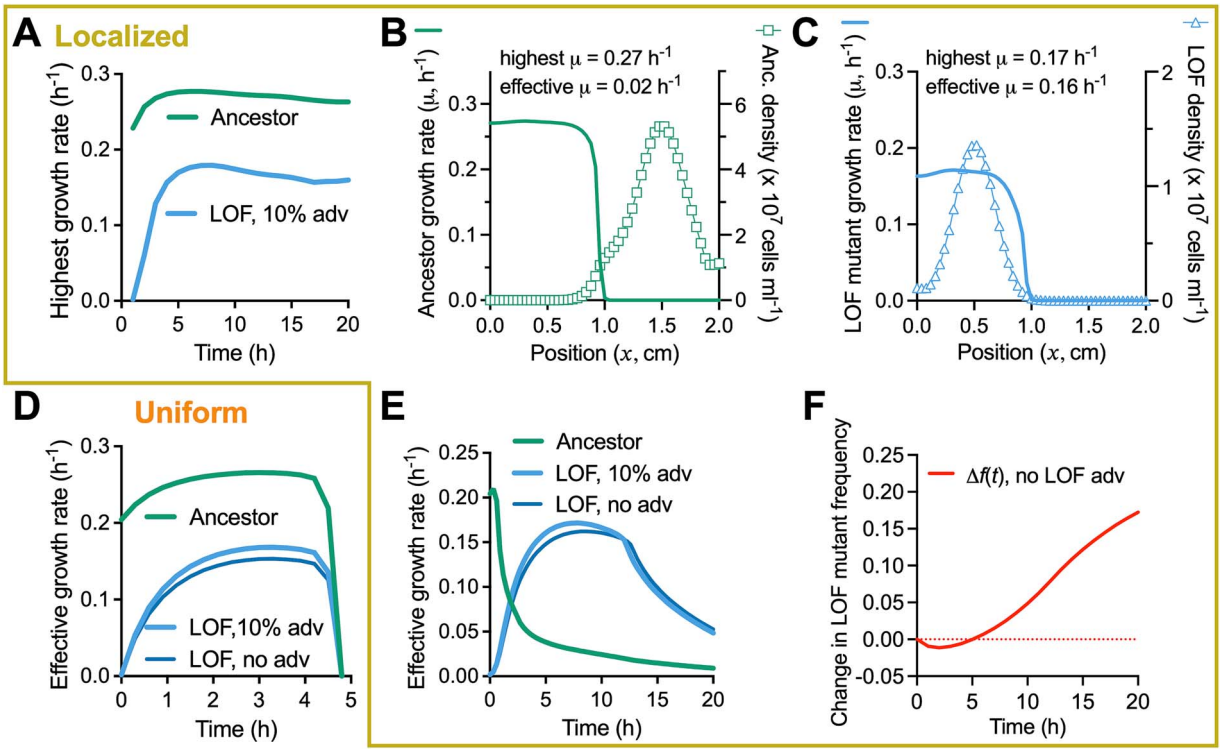

Figure 6. Segregation from the ancestor allows the LOF mutant to be enriched without an intrinsic maximum growth rate (μ^i_{max}) advantage when colocalized with the producer; all graphs are from simulated cocultures using an initial LOF mutant frequency f_0 of 0.061 (*V. natriegens* populations only); all localized conditions (A-C,E,F) used initial population spatial distributions as in Fig. 5A where the producer and LOF inoculums are colocalized ($\sigma = 0.2$); (A) the highest growth rates in the spatial domain; (B, C) a cross-section across the domain at t = 10 h and y = 1 cm shows that the highest growth rate does not always occur at the same location as the highest cell density; to compare growth rates, we therefore adopted an effective growth rate ($\mu^i_{effective}(t)$), which is a spatially averaged growth rate weighed by cell density (Supplementary material, Eqs. (22)–(23)); effective growth rates with uniform (D) or localized conditions (E) when the LOF mutant does, and does not have a 10% maximum growth rate advantage (adv) over the ancestor (Anc); (F) change in frequency for the conditions in (E) when the LOF mutant does not have a maximum growth advantage; change in frequency was calculated from time integrals of the effective growth rates (Supplementary material, Eq. (34) and Fig. S9).

Glucose was also depleted more slowly on the opposite side of the vial (Fig. 5E). Thus, inoculating populations on opposite sides of the vial should allow for interactions from partially overlapping populations, but with less local competition. We co-inoculated the producer and the LOF mutant on one side of the vial and the ancestor on the other side (Fig. 5C). In agreement with the simulations, the LOF mutant was enriched, with predicted coexistence with the ancestor ((x,0) = 0.77; 95% CI: 0.64 to 0.98; Fig. 5F). The final LOF mutant frequency was also significantly higher compared to that in static liquid (Fig. 5G, *V. natriegens* populations only; the producer was the dominant species, making up ~99% of the total population, Fig. 5H).

Coexistence differs from the BQH prediction of ancestor extinction [1]. We thus investigated whether our results met the BQH criterion of a LOF mutant fitness advantage [1], for which we used growth rate. The simulated NH_4^+ concentration never exceeded the half-saturation constant (*km*) (Fig. S8), explaining why the highest growth rate $(\mu^i(\vec{r}, t))$ at any location in the spatial domain for the LOF mutant never exceeded that of the ancestor (Fig. 6A, S8).

Using growth rate as the fitness metric in numerical simulations with non-uniform spatial conditions can be misleading; the calculated growth rate at a given point in time and space can be high because of nutrient availability but cells might be absent to take advantage of local conditions (Fig. 6B, C). We therefore examined effective growth rate ($\mu^i_{effective}(t)$), a spatially averaged growth rate weighted by cell density (Supplementary material).

Under uniform conditions, the effective ancestor growth rate was always higher than that of the LOF mutant (Fig. 6D). However, for localized conditions, the LOF mutant achieved a higher effective growth rate for most of the simulation, explaining its enrichment (Fig. 6E). To assess whether the encoded LOF mutant maximum growth rate (μ^i_{max}) advantage, afforded by the LOF mutation, contributed to this outcome, we simulated the same conditions with no maximum growth rate advantage. In this case, the effective LOF mutant growth rate was lower, but not enough to affect population outcomes (Fig. 6D–F; change in fitness was determined from the time integral of the effective growth rate; Fig. S9). Thus, our results suggest that the LOF mutant enrichment was due to the initial partial segregation from the ancestor, leading to local glucose depletion that prevented invasion by the ancestor (Fig. S8). In other words, spatial conditions, rather than an intrinsic fitness advantage from gene loss, led to the enrichment of the LOF mutant.

LOF mutant enrichment is determined by the degree of segregation from the ancestor

Based on the above results we hypothesized that LOF mutant enrichment would depend on the degree of segregation from the ancestor. We thus simulated inoculation sites as above and increased population overlap by modifying the standard deviation of the Gaussian distributions (σ) for all populations (Fig. 7A); the LOF mutant and producer peaks were always colocalized and thus both experienced increasing initial overlap with the ancestor

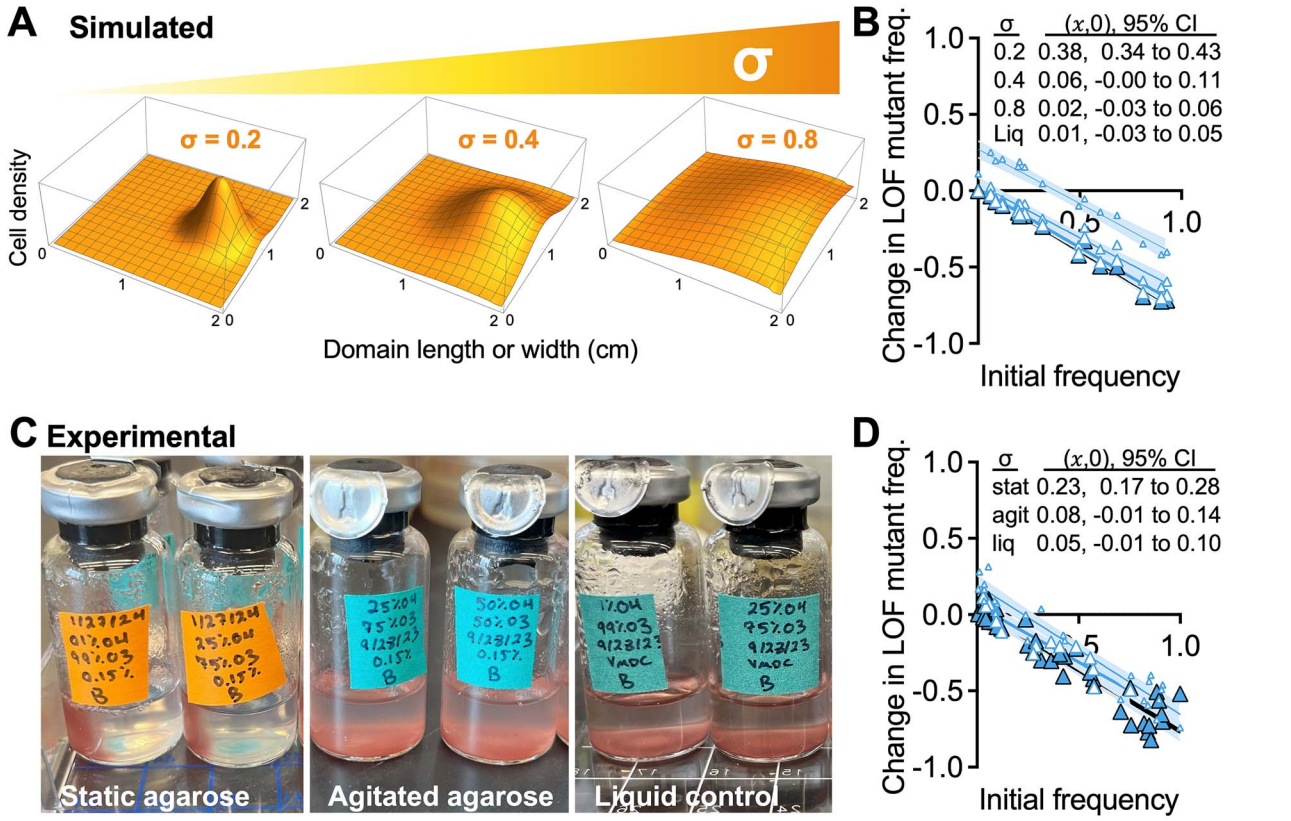

Figure 7. Increasing population overlap prevents enrichment of the LOF mutant; (A) initial population distribution varied by σ (standard deviation of Gaussian distributed inoculum); the y-scales are arbitrary to demonstrate how increasing σ both flattens and broadens the initial population distribution; (B) simulated IFR assays using different σ for all populations to affect overlap between the ancestor and LOF populations; inoculum locations were the same as in Fig. 5, where the LOF mutant and producer are colocalized; (C) experimental conditions varied σ by not disturbing 0.15% agarose (stat), agitating agarose by stirring before inoculation (agit), or using static liquid (liq); the degree of localized populations is evident from growth of pigmented *R. palustris* after 6 days; (D) IFR results from (C) cocultures were only mixed before sampling; (B, D) each point is from an individual experimental or simulated coculture; initial LOF mutant frequencies were the same for experimental and simulated cocultures (initial frequency range = 3.1%–91.4% using *V. natriegens* populations only); x-intercept and 95% CI error bands were determined using linear regression analysis.

population. Increasing σ led to a decrease in the IFR x-intercept (Fig. 7B); for $\sigma > 0.4$, IFR plots resembled uniform conditions, highlighting the importance of LOF mutant segregation from the ancestor.

To test the simulated predictions, we agitated 0.15% agarose by stirring to fragment the polymer and thereby widen initial distributions at inoculation sites (Fig. 7C). Consistent with the simulated results, agitating the agarose (increasing σ), moved the IFR results to resemble uniform conditions (Fig. 7D). The sensitivity of the matrix to disturbance might also explain the different values from different IFR assays (Fig. 5D vs Fig. 7D) compared to static liquid that always gave x-intercept values that were not significantly different from zero (Fig. S10). Our results indicate that less spatial overlap with the ancestor is essential for LOF mutant enrichment, even when the mutant and producer are colocalized.

LOF mutant enrichment does not require producer colocalization

The above tests always colocalized the LOF mutant with the producer. We questioned whether colocalization of these populations was required for LOF mutant enrichment. We thus simulated IFR conditions with the producer and ancestor colocalized and segregated from the LOF mutant (Fig. 8A; $\sigma = 0.2$). The x-intercept again suggested LOF mutant coexistence with the ancestor, but at a lower equilibrium frequency ((x,0) = 0.06; 95% CI: 0.03 to 0.10; Fig. 8B). This result was confirmed experimentally by inoculating populations in a similar spatial arrangement in 0.15% agarose ((x,0) = 0.07; 95% CI: 0.04 to 0.19; Fig. 8C). Again, this result was not dependent on the LOF mutant maximum growth rate advantage (Fig. 8D). Overall, our results suggest that segregation from the ancestor is more important for LOF mutant enrichment than producer colocalization, provided there is still sufficient access to NH_4^+ from the producer.

Discussion

We used an experimental coculture and a mathematical model to test the BQH prediction that loss of nitrogenase would be beneficial [1]. Beneficial nitrogenase loss did not seem feasible given that low extracellular NH_4^+ would prevent a higher growth rate than that with N_2 (Fig. 1B, C). Indeed, the LOF mutant was consistently outcompeted by the ancestor under uniform conditions (Fig. 2, Fig. S10). However, segregation from the ancestor, while maintaining access to NH_4^+ from the producer, led to LOF mutant enrichment (Fig. 4-8). Although we observed nitrogenase mutant enrichment, the outcome differed from BQH predictions in two ways [1]: (i) the data suggested mutant coexistence with the ancestor (Fig. 4-8; IFR (x,0) between 0 and 1), and (ii) a maximum growth rate (μ^i_{max}) advantage from gene loss was not required (Figs. 6, 8). Thus, a LOF nitrogenase mutant need not be a beneficiary nor a cheater to be enriched in the above spatial conditions.

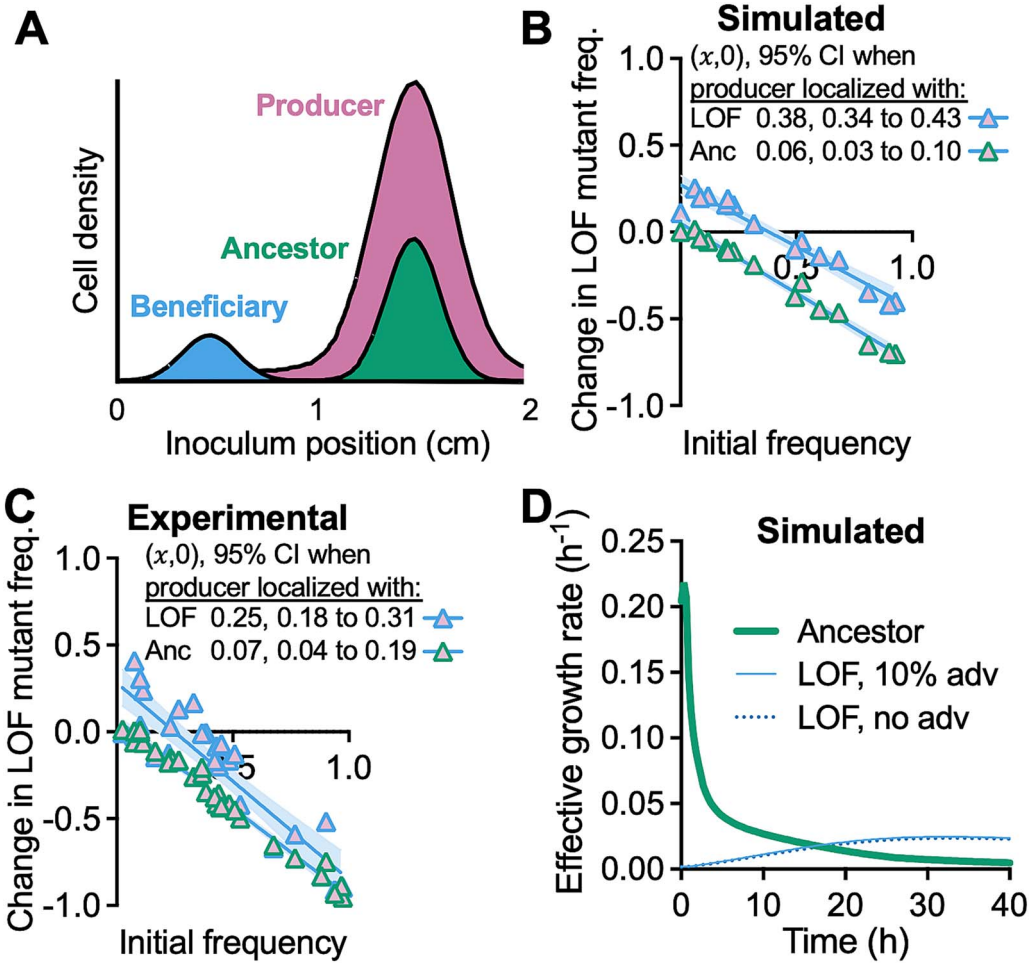

Figure 8. The LOF mutant can be enriched even when segregated from colocalized ancestor and producer populations; (A) initial population distributions (not to scale); (B,C) simulated (B) and experimental (C) IFR assays comparing conditions where either the LOF mutant or the ancestor is colocalized with the producer; each point is from an individual simulated or experimental coculture; initial LOF mutant frequencies were the same for experimental and simulated cocultures (initial frequency range = 0.1%–92.8% using *V. natriegens* populations only); experimental cocultures were only mixed before sampling; x-intercept and 95% CI error bands were determined using linear regression analysis; (D) effective growth rates for a simulation where the initial populations are distributed as in (A) with an initial LOF mutant frequency $f_0 = 0.061$.

Partial privatization and LOF mutant outcomes

There are likely other cases where sub-saturating cross-fed nutrients under uniform conditions would favor the ancestor over a LOF mutant. However, the privatization level of a cross-fed resource could flip this outcome, even under uniform conditions [2, 43, 63–65, 67, 68]. For example, others have predicted that intracellularly-generated NH_4^+ from N_2 fixation is less likely to support LOF mutants than extracellular iron-scavenging siderophores, for which ancestors and LOF mutants have equal access [63]. This finding agrees with our hypothetical scenario where we simulated extracellular NH_4^+ production and observed LOF mutant dominance (Fig. 3). Privatization might help explain why there are few reports of spontaneous auxotroph emergence during long-term cross-feeding of intracellularly generated compounds; in one example, emergent amino acid auxotrophs appeared to be transient [10]. However, in examples of less-privatized detoxification services, spontaneous LOF mutants appeared to be stable [17, 18]. Still, engineered pairings of amino acid auxotrophs and producers suggest that beneficial fitness outcomes are possible [69–71]. One possibility is that these cases involved easily overlooked but important spatial organization, like microscopic cell clusters [28].

Microbial community structure can accommodate disadvantageous gene loss

The nitrogenase LOF mutation in our study is clearly disadvantageous. Thus, the mutant was neither a cheater nor a beneficiary, both of which imply a fitness advantage from gene loss. Whereas a LOF cheater would benefit from emergence within a large exploitable ancestor population [24, 27, 29, 34–36], enrichment of a LOF nitrogenase mutant instead depended on a level of segregation from its competitive ancestor. Our findings resemble others where a less-fit mutant succeeded at the edge of the ancestor population where competition was lower [39]. But how can a less-fit LOF mutant escape its ancestor?

Segregation can be achieved through either dispersal of the LOF mutant or the ancestor. For example, three bacterial species cocultured in a nutrient rich environment could only coexist in a biofilm if there was biased dispersal of the dominant competitor [72]. Whereas we used non-motile strains to provide more control over location, microbial motility can also influence cooperator-competitor interactions. For example, competition against a cheater was improved when an amino acid cross-feeding bacterium was motile [29]. Motility also allowed for slower-growing cooperative strains to increase in frequency relative to

a cheater in swim agar [73]. Non-motile cells can also escape communities via fluid flow (advection) [74]. Transient flow across a surface can rapidly isolate cells, albeit at a low frequency in lab conditions [75]. Other forms of community disruption or bottlenecking can also lead to segregation and benefit a slow-growing subpopulation [76, 77].

With prolonged segregation from the ancestor and access to a cross-feeding partner, further genetic diversification can occur including obligate dependencies through additional LOF mutations [5, 6]. These events could contribute to genome streamlining, which the BQH can partially address [1, 78, 79]. But what mechanisms would enrich for additional LOF mutations? Although segregation from competitors can lead to the enrichment of a LOF mutant, it seems improbable that successive mutations would always coincide with both segregation from the ancestor and access to a cross-feeding partner. More likely, segregation from the ancestor is just one factor contributing to the origin and maintenance of gene loss-associated cross-feeding, along with mutations that impart competitive advantages, like those described by the BQH. Our findings underscore that environmental features that influence spatial community structure are important to consider in the evolution of cooperative phenotypes that might otherwise seem to defy evolutionary theory.

Acknowledgements

We thank A. Stoner for assistance constructing CGA4039 and N. Haas for constructing NH003 and NH004. We thank C. Love for piloting early experiments and M. Di Salvo and K. Locey for useful discussions during the initial stages of the project. We also thank the McKinlay lab and the local *Vibrio* group for helpful advice.

Supplementary material

Supplementary material is available at *The ISME Journal* online.

Conflicts of interest

None declared.

Funding

This work was supported in part by the US Army Research Office grants W911NF-14-1-0411, the National Science Foundation CAREER award MCB-1749489, the GEMS Biology Integration Institute (NSF DBI Biology Integration Institutes Program, Award #2022049) and Indiana University. Supercomputing resources were supported in part by Lilly Endowment, Inc., through its support for the IU Pervasive Technology Institute.

Data availability

All data for this study are in this article and its supplementary information files.

References

1. Morris JJ, Lenski RE, Zinser ER. The Black Queen Hypothesis: evolution of dependencies through adaptive gene loss. *mBio* 2012;**3**:e00036–12. https://doi.org/10.1128/mBio.00036-12
2. Morris JJ. Black Queen evolution: the role of leakiness in structuring microbial communities. *Trends Genet* 2015;**31**:475–82. https://doi.org/10.1016/j.tig.2015.05.004
3. Ghoul M, Griffin AS, West SA. Toward an evolutionary definition of cheating. *Evolution* 2014;**68**:318–31. https://doi.org/10.1111/evo.12266
4. Smith P, Schuster M. Public goods and cheating in microbes. *Curr Biol* 2019;**29**:R442–7. https://doi.org/10.1016/j.cub.2019.03.001
5. D'Souza G, Shitut S, Preussger D. *et al.* Ecology and evolution of metabolic cross-feeding interactions in bacteria. *Nat Prod Rep* 2018;**35**:455–88. https://doi.org/10.1039/C8NP00009C
6. Pande S, Kost C. Bacterial unculturability and the formation of intercellular metabolic networks. *Trends Microbiol* 2017;**25**:349–61. https://doi.org/10.1016/j.tim.2017.02.015
7. Wienhausen G, Moraru C, Bruns S. *et al.* Ligand cross-feeding resolves bacterial vitamin B_{12} auxotrophies. *Nature* 2024;**629**:886–92. https://doi.org/10.1038/s41586-024-07396-y
8. Guseva K, Mohrlok M, Alteio L. *et al.* Bacteria face trade-offs in the decomposition of complex biopolymers. *PLoS Comput Biol* 2024;**20**:e1012320. https://doi.org/10.1371/journal.pcbi.1012320
9. Rodriguez-Gijon A, Buck M, Andersson AF. *et al.* Linking prokaryotic genome size variation to metabolic potential and environment. *ISME Commun* 2023;**3**:25. https://doi.org/10.1038/s43705-023-00231-x
10. D'Souza G, Kost C. Experimental evolution of metabolic dependency in bacteria. *PLoS Genet* 2016;**12**:e1006364. https://doi.org/10.1371/journal.pgen.1006364
11. Dykhuizen D. Selection for tryptophan auxotrophs of *Escherichia coli* in glucose-limited chemostats as a test of the energy conservation hypothesis of evolution. *Evolution* 1978;**32**:125–50. https://doi.org/10.1111/j.1558-5646.1978.tb01103.x
12. D'Souza G, Waschina S, Pande S. *et al.* Less is more: selective advantages can explain the prevalent loss of biosynthetic genes in bacteria. *Evolution* 2014;**68**:2559–70. https://doi.org/10.1111/evo.12468
13. Helliwell KE, Collins S, Kazamia E. *et al.* Fundamental shift in vitamin B_{12} eco-physiology of a model alga demonstrated by experimental evolution. *ISME J* 2015;**9**:1446–55. https://doi.org/10.1038/ismej.2014.230
14. Dumas Z, Kümmerli R. Cost of cooperation rules selection for cheats in bacterial metapopulations. *J Evol Biol* 2012;**25**:473–84. https://doi.org/10.1111/j.1420-9101.2011.02437.x
15. Harrison F, Paul J, Massey RC. *et al.* Interspecific competition and siderophore-mediated cooperation in *Pseudomonas aeruginosa*. *ISME J* 2008;**2**:49–55. https://doi.org/10.1038/ismej.2007.96
16. Figueiredo ART, Wagner A, Kümmerli R. Ecology drives the evolution of diverse social strategies in *Pseudomonas aeruginosa*. *Mol Ecol* 2021;**30**:5214–28. https://doi.org/10.1111/mec.16119
17. Morris JJ, Papoulis SE, Lenski RE. Coexistence of evolving bacteria stabilized by a shared Black Queen function. *Evolution* 2014;**68**:2960–71. https://doi.org/10.1111/evo.12485
18. Adkins-Jablonsky SJ, Clark CM, Papoulis SE. *et al.* Market forces determine the distribution of a leaky function in a simple microbial community. *Proc Natl Acad Sci USA* 2021;**118**:e2109813118. https://doi.org/10.1073/pnas.2109813118
19. Bueno Batista M, Dixon R. Manipulating nitrogen regulation in diazotrophic bacteria for agronomic benefit. *Biochem Soc Trans* 2019;**47**:603–14. https://doi.org/10.1042/BST20180342
20. Kleiner D. Bacterial ammonium transport. *FEMS Microbiol Lett* 1985;**32**:87–100. https://doi.org/10.1111/j.1574-6968.1985.tb01185.x
21. Walter A, Gutknecht J. Permeability of small nonelectrolytes through lipid bilayer membranes. *J Membr Biol* 1986;**90**:207–17. https://doi.org/10.1007/BF01870127
22. Fritts RK, Bird JT, Behringer MG. *et al.* Enhanced nutrient uptake is sufficient to drive emergent cross-feeding between bacteria

in a synthetic community. *ISME J* 2020;**14**:2816–28. https://doi.org/10.1038/s41396-020-00737-5
23. LaSarre B, McCully AL, Lennon JT. *et al.* Microbial mutualism dynamics governed by dose-dependent toxicity of cross-fed nutrients. *ISME J* 2017;**11**:337–48. https://doi.org/10.1038/ismej.2016.141
24. Pande S, Kaftan F, Lang S. *et al.* Privatization of cooperative benefits stabilizes mutualistic cross-feeding interactions in spatially structured environments. *ISME J* 2016;**10**:1413–23. https://doi.org/10.1038/ismej.2015.212
25. Harcombe W. Novel cooperation experimentally evolved between species. *Evolution* 2010;**64**:2166–72. https://doi.org/10.1111/j.1558-5646.2010.00959.x
26. Kim HJ, Boedicker JQ, Choi JW. *et al.* Defined spatial structure stabilizes a synthetic multispecies bacterial community. *Proc Natl Acad Sci USA* 2008;**105**:18188–93. https://doi.org/10.1073/pnas.0807935105
27. Momeni B, Waite AJ, Shou W. Spatial self-organization favors heterotypic cooperation over cheating. *eLife* 2013;**2**:e00960. https://doi.org/10.7554/eLife.00960
28. Preussger D, Giri S, Muhsal LK. *et al.* Reciprocal fitness feedbacks promote the evolution of mutualistic cooperation. *Curr Biol* 2020;**30**:3580–3590.e7. https://doi.org/10.1016/j.cub.2020.06.100
29. Scarinci G, Sourjik V. Impact of direct physical association and motility on fitness of a synthetic interkingdom microbial community. *ISME J* 2023;**17**:371–81. https://doi.org/10.1038/s41396-022-01352-2
30. Nadell CD, Drescher K, Foster KR. Spatial structure, cooperation and competition in biofilms. *Nat Rev Microbiol* 2016;**14**:589–600. https://doi.org/10.1038/nrmicro.2016.84
31. Dal Co A, van Vliet S, Kiviet DJ. *et al.* Short-range interactions govern the dynamics and functions of microbial communities. *Nat Ecol Evol* 2020;**4**:366–75. https://doi.org/10.1038/s41559-019-1080-2
32. Kümmerli R, Griffin AS, West SA. *et al.* Viscous medium promotes cooperation in the pathogenic bacterium *Pseudomonas aeruginosa*. *Proc Biol Sci* 2009;**276**:3531–8. https://doi.org/10.1098/rspb.2009.0861
33. Kreft JU. Biofilms promote altruism. *Microbiology* 2004;**150**:2751–60. https://doi.org/10.1099/mic.0.26829-0
34. Drescher K, Nadell Carey D, Stone Howard A. *et al.* Solutions to the public goods dilemma in bacterial biofilms. *Curr Biol* 2014;**24**:50–5. https://doi.org/10.1016/j.cub.2013.10.030
35. Stump SM, Johnson EC, Klausmeier CA. Local interactions and self-organized spatial patterns stabilize microbial cross-feeding against cheaters. *J R Soc Interface* 2018;**15**:20170822. https://doi.org/10.1098/rsif.2017.0822
36. Germerodt S, Bohl K, Lück A. *et al.* Pervasive selection for cooperative cross-feeding in bacterial communities. *PLoS Comp Biol* 2016;**12**:e1004986. https://doi.org/10.1371/journal.pcbi.1004986
37. Behringer MG, Ho WC, Meraz JC. *et al.* Complex ecotype dynamics evolve in response to fluctuating resources. *mBio* 2022;**13**:e0346721. https://doi.org/10.1128/mbio.03467-21
38. Vallespir Lowery N, Ursell T. Structured environments fundamentally alter dynamics and stability of ecological communities. *Proc Natl Acad Sci USA* 2019;**116**:379–88. https://doi.org/10.1073/pnas.1811887116
39. Burton OJ, Travis JM. The frequency of fitness peak shifts is increased at expanding range margins due to mutation surfing. *Genetics* 2008;**179**:941–50. https://doi.org/10.1534/genetics.108.087890
40. Wright S. Evolution in Mendelian populations. *Genetics* 1931;**16**:97–159. https://doi.org/10.1093/genetics/16.2.97
41. Dalia TN, Hayes CA, Stolyar S. *et al.* Multiplex genome editing by natural transformation (MuGENT) for synthetic biology in *Vibrio natriegens*. *ACS Synth Biol* 2017;**6**:1650–5. https://doi.org/10.1021/acssynbio.7b00116
42. Dalia TN, Yoon SH, Galli E. *et al.* Enhancing multiplex genome editing by natural transformation (MuGENT) via inactivation of ssDNA exonucleases. *Nucleic Acids Res* 2017;**45**:7527–37. https://doi.org/10.1093/nar/gkx496
43. McCully AL, LaSarre B, McKinlay JB. Recipient-biased competition for an intracellularly generated cross-fed nutrient is required for coexistence of microbial mutualists. *mBio* 2017;**8**:e01620–17. https://doi.org/10.1128/mBio.01620-17
44. Mazny BE, Sheff OF, LaSarre B. *et al.* Complete genome sequence of *Rhodopseudomonas palustris* CGA0092 and corrections to the *R. palustris* CGA009 genome sequence. *Microbiol Resour Announc* 2023;**12**:e0128522. https://doi.org/10.1128/mra.01285-22
45. Fritts RK, LaSarre B, Stoner AM. *et al.* A Rhizobiales-specific unipolar polysaccharide adhesin contributes to *Rhodopseudomonas palustris* biofilm formation across diverse photoheterotrophic conditions. *Appl Environ Microbiol* 2017;**83**:e03035–16. https://doi.org/10.1128/aem.03035-16
46. McKinlay JB, Harwood CS. Carbon dioxide fixation as a central redox cofactor recycling mechanism in bacteria. *Proc Natl Acad Sci USA* 2010;**107**:11669–75. https://doi.org/10.1073/pnas.1006175107
47. Oda Y, Samanta SK, Rey FE. *et al.* Functional genomic analysis of three nitrogenase isozymes in the photosynthetic bacterium *Rhodopseudomonas palustris*. *J Bacteriol* 2005;**187**:7784–94. https://doi.org/10.1128/JB.187.22.7784-7794.2005
48. Fritts RK. The physiology, mechanisms, and evolution of bacterial cross-feeding and nutrient acquisition. *PhD. Dissertation.* Indiana University Department of Biology 2019.
49. Pelletier DA, Hurst GB, Foote LJ. *et al.* A general system for studying protein–protein interactions in gram-negative bacteria. *J Proteome Res* 2008;**7**:3319–28. https://doi.org/10.1021/pr8001832
50. Rey FE, Oda Y, Harwood CS. Regulation of uptake hydrogenase and effects of hydrogen utilization on gene expression in *Rhodopseudomonas palustris*. *J Bacteriol* 2006;**188**:6143–52. https://doi.org/10.1128/jb.00381-06
51. LaSarre B, Morlen R, Neumann GC. *et al.* Nitrous oxide reduction by two partial denitrifying bacteria requires denitrification intermediates that cannot be respired. *Appl Environ Microbiol* 2024;**90**:e0174123. https://doi.org/10.1128/aem.01741-23
52. McKinlay JB, Zeikus JG, Vieille C. Insights into *Actinobacillus succinogenes* fermentative metabolism in a chemically defined growth medium. *Appl Environ Microbiol* 2005;**71**:6651–6. https://doi.org/10.1128/aem.71.11.6651-6656.2005
53. Hammarlund SP, Chacón JM, Harcombe WR. A shared limiting resource leads to competitive exclusion in a cross-feeding system. *Environ Microbiol* 2019;**21**:759–71. https://doi.org/10.1111/1462-2920.14493
54. Sander R. Compilation of Henry's law constants (version 5.0.0) for water as solvent. *Atmos Chem Phys* 2023;**23**:10901–2440. https://doi.org/10.5194/acp-23-10901-2023
55. Khademi S, O'Connell J 3rd, Remis J. *et al.* Mechanism of ammonia transport by Amt/MEP/Rh: structure of AmtB at 1.35 A. *Science* 2004;**305**:1587–94. https://doi.org/10.1126/science.1101952
56. Burns RC, Hardy RW. Purification of nitrogenase and crystallization of its Mo-Fe protein. *Methods Enzymol* 1972;**24**:480–96. https://doi.org/10.1016/0076-6879(72)24094-0

57. Chesson P. Mechanisms of maintenance of species diversity. *Annu Rev Ecol Syst* 2000;**31**:343–66. https://doi.org/10.1146/annurev.ecolsys.31.1.343
58. Grainger TN, Levine JM, Gilbert B. The invasion criterion: a common currency for ecological research. *Trends Ecol Evol* 2019;**34**:925–35. https://doi.org/10.1016/j.tree.2019.05.007
59. Barney BM, Eberhart LJ, Ohlert JM. *et al.* Gene deletions resulting in increased nitrogen release by *Azotobacter vinelandii*: application of a novel nitrogen biosensor. *Appl Environ Microbiol* 2015;**81**:4316–28. https://doi.org/10.1128/AEM.00554-15
60. Dietz BR, Olszewski NE, Barney BM. Enhanced extracellular ammonium release in the plant endophyte *Gluconacetobacter diazotrophicus* through genome editing. *Microbiol Spectr* 2024;**12**:e0247823. https://doi.org/10.1128/spectrum.02478-23
61. Narula N, Lakshminarayana K, Tauro P. Ammonia excretion by *Azotobacter chroococcum*. *Biotechnol Bioeng* 1981;**93**:205–9. https://doi.org/10.1002/bit.260230224
62. Milo R, Jorgensen P, Moran U. *et al.* BioNumbers–the database of key numbers in molecular and cell biology. *Nucleic Acids Res* 2010;**38**:D750–3. https://doi.org/10.1093/nar/gkp889
63. Lerch BA, Smith DA, Koffel T. *et al.* How public can public goods be? Environmental context shapes the evolutionary ecology of partially private goods. *PLoS Comput Biol* 2022;**18**:e1010666. https://doi.org/10.1371/journal.pcbi.1010666
64. Hoek TA, Axelrod K, Biancalani T. *et al.* Resource availability modulates the cooperative and competitive nature of a microbial cross-feeding mutualism. *PLoS Biol* 2016;**14**:e1002540. https://doi.org/10.1371/journal.pbio.1002540
65. Estrela S, Morris JJ, Kerr B. Private benefits and metabolic conflicts shape the emergence of microbial interdependencies. *Environ Microbiol* 2016;**18**:1415–27. https://doi.org/10.1111/1462-2920.13028
66. Gore J, Youk H, van Oudenaarden A. Snowdrift game dynamics and facultative cheating in yeast. *Nature* 2009;**459**:253–6. https://doi.org/10.1038/nature07921
67. Shao J, Rong N, Wu Z. *et al.* Siderophore-mediated iron partition promotes dynamical coexistence between cooperators and cheaters. i*Science* 2023;**26**:107396. https://doi.org/10.1016/j.isci.2023.107396
68. Raj N, Saini S. Increased privatization of a public resource leads to spread of cooperation in a microbial population. *Microbiol Spectr* 2024;**12**:e0235823. https://doi.org/10.1128/spectrum.02358-23
69. Pande S, Merker H, Bohl K. *et al.* Fitness and stability of obligate cross-feeding interactions that emerge upon gene loss in bacteria. *ISME J* 2013;**8**:953–62. https://doi.org/10.1038/ismej.2013.211
70. Mee MT, Collins JJ, Church GM. *et al.* Syntrophic exchange in synthetic microbial communities. *Proc Natl Acad Sci USA* 2014;**111**:E2149–56. https://doi.org/10.1073/pnas.1405641111
71. Wintermute EH, Silver PA. Emergent cooperation in microbial metabolism. *Mol Syst Biol* 2010;**6**:407. https://doi.org/10.1038/msb.2010.66
72. Holt JD, Schultz D, Nadell CD. Dispersal of a dominant competitor can drive multispecies coexistence in biofilms. *Curr Biol* 2024;**34**:4129–4142.e4. https://doi.org/10.1016/j.cub.2024.07.078
73. Bruger EL, Waters CM. Maximizing growth yield and dispersal via quorum sensing promotes cooperation in *Vibrio* bacteria. *Appl Environ Microbiol* 2018;**84**:e00402–18. https://doi.org/10.1128/AEM.00402-18
74. Rossy T, Nadell CD, Persat A. Cellular advective-diffusion drives the emergence of bacterial surface colonization patterns and heterogeneity. *Nat Commun* 2019;**10**:2471. https://doi.org/10.1038/s41467-019-10469-6
75. Weaver AA, Bolster D, Madukoma CS. *et al.* Transient surface hydration impacts biogeography and intercellular interactions of non-motile bacteria. *Appl Environ Microbiol* 2021;**87**:e03067–20. https://doi.org/10.1128/AEM.03067-20
76. Chuang JS, Rivoire O, Leibler S. Simpson's paradox in a synthetic microbial system. *Science* 2009;**323**:272–5. https://doi.org/10.1126/science.1166739
77. Cremer J, Melbinger A, Frey E. Growth dynamics and the evolution of cooperation in microbial populations. *Sci Rep* 2012;**2**:281. https://doi.org/10.1038/srep00281
78. Giovannoni SJ, Cameron Thrash J, Temperton B. Implications of streamlining theory for microbial ecology. *ISME J* 2014;**8**:1553–65. https://doi.org/10.1038/ismej.2014.60
79. Koskiniemi S, Sun S, Berg OG. *et al.* Selection-driven gene loss in bacteria. *PLoS Genet* 2012;**8**:e1002787. https://doi.org/10.1371/journal.pgen.1002787

The ISME Journal, 2025, **19(1)**, wraf131
https://doi.org/10.1093/ismejo/wraf131
Original Article